Supplemental materials

Epichaperome inhibition targets *TP53*-mutant AML and AML stem/progenitor cells

Bing Z. Carter,[1] Po Yee Mak,[1] Muharrem Muftuoglu,[1] Wenjing Tao,[1] Baozhen Ke,[1] Jingqi Pei,[1] Andrea D. Bedoy,[1] Lauren B. Ostermann,[1] Yuki Nishida,[1] Sevinj Isgandarova,[2] Mary Sobieski,[3] Nghi Nguyen,[3] Reid T. Powell,[3] Margarita Martinez-Moczygemba,[2] Clifford Stephan,[3] Mahesh Basyal,[1] Naveen Pemmaraju,[4] Steffen Boettcher,[5] Benjamin L. Ebert,[6] Elizabeth J. Shpall,[7] Barbara Wallner,[8] Robert A. Morgan,[8] Georgios I. Karras,[9;10] Ute M. Moll,[11] and Michael Andreeff[1]

Supplemental methods

High-throughput drug screening: We performed high-throughput drug screening to identify compounds that kill cells independent of *TP53* mutation status. *TP53*-wild type (WT) and -mutant (R175H, R248Q) Molm13 cells[1] were seeded into black 384-well plates (Greiner Bio-One) using a Multidrop Combi nL reagent dispenser (ThermoFisher Scientific) in media containing Draq7 (DR710HC, Biostatus), a DNA dye that only stains the nuclei of dead and permeabilized cells. The Approved Drug collection (TargetMol) containing 2040 drugs and 358 commercially available compounds from the Broad Institute Informer Set[2] (Supplemental Table 2) were transferred into the cell-containing wells using an Echo 550 acoustic dispensing platform (Labcyte). Each plate also contained DMSO (0.1%, v/v, n=8) and positive control wells (17-AAG [1 μM], n=8) that were used to calculate a Z' factor. Additional controls were included on all plates to control for both intra- and inter-assay variability. A 17-AAG (5-350 nM) and a PU-H71 (3 nM-1μM) concentration response curve, each runs with technical duplicates, were used to determine the minimum significance ratio statistic. At the time of drug addition, a separate untreated plate was analyzed by flow cytometry for cell number and viability within 2-4 h of plating to establish a baseline cell count for subsequent growth and cytotoxicity analysis after 72 h of drug exposure.[3] 12 μL of media (total 50 μL) were sampled from each well using a ZE5 high throughput flow cytometer (BioRad). Plates were shaken for 15 s initially and 5 s after 2 columns. Cells were first gated using FlowJo 10.8.1 (BD) by identifying the major population from a forward vs side scatter graph. The viable population was quantified by selecting the Draq7 negative population using the built in peak detection algorithm. The viable cell count was normalized to the growth rate of negative controls. The FlowJo analysis was fully automated using Pipeline Pilot (Dassault Systemes Biovia). We observed median Z' values for *TP53*-WT, *TP53*-R17H, and *TP53*-R248Q Molm13 as 0.83±0.05, 0.82±0.05, and 0.80±0.06, respectively, demonstrating a highly consistent and robust analysis method.

High-parametric cell death assay: Cells treated with PU-H71 at specified concentrations were harvested, washed, suspended in PBS, and labeled with live/dead cell aqua dye (Tonbo Biosciences). Cells were then fixed, permeabilized with Foxp3 staining buffer set (ThemoFisher) and stained with a collection of antibodies to detect various cell death modes and cell stress responses, including ATF4 (Proteintech), p21 (Cell Signaling Technology), RIP3 (Santa Cruz Biotechnology, Inc.), γ-H2AX (BioLegend), Ki67 (BD Biosciences), LC3B (Cell Signaling Technology), cleaved caspase-3 and cleaved PARP (both from BD Biosciences) and measured by a Cytoflex flow cytometer equipped with 4 lasers (Beckman Coulter, Miami, USA). Data analysis was performed using FlowJo v.10.8.1. software (BD Biosciences). We excluded debris, gated on singlets, and exported events including both live and dead cells for subsequent high-dimensional analysis. Pooled cells from all experimental conditions were subjected to UMAP dimensional reduction by all features (including LC3B, RIP3, ATF4, Ki67, γ-H2AX, p21, cleaved

caspase-3, cleaved PARP and live-dead aqua dye) and FlowSOM clustering was performed using the omiq.ai platform. Scaled expression values were used to generate single-cell protein expression heatmaps and violin plots, and perform differential expression analysis in R software version 4.0.0 (R Foundation for Statistical Computing, Vienna, Austria; https://www.R-project.org) as previously described[4]. We utilized the Seurat package[5] to cluster *TP53*-WT, -KO, and -mutant (R175H and Y220C) Molm13 cells treated with PU-H71 using the FlowSOM cluster frequencies. UMAP embedding based on four principal components was used to separate different experimental conditions.

Supplemental Figures

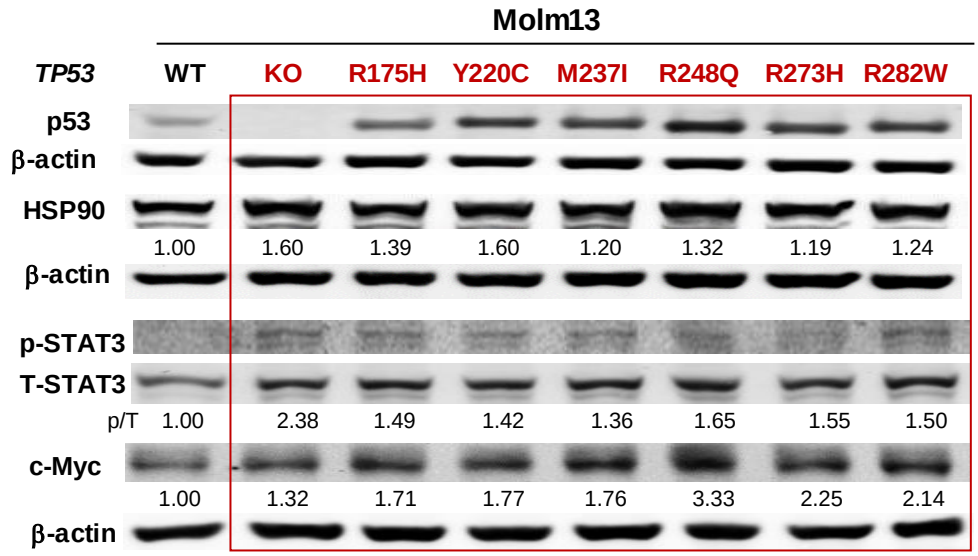

Supplemental Figure S1. Protein expression in *TP53*-WT, -KO, and -mutant Molm13 cells. The levels were determined by Western blotting.

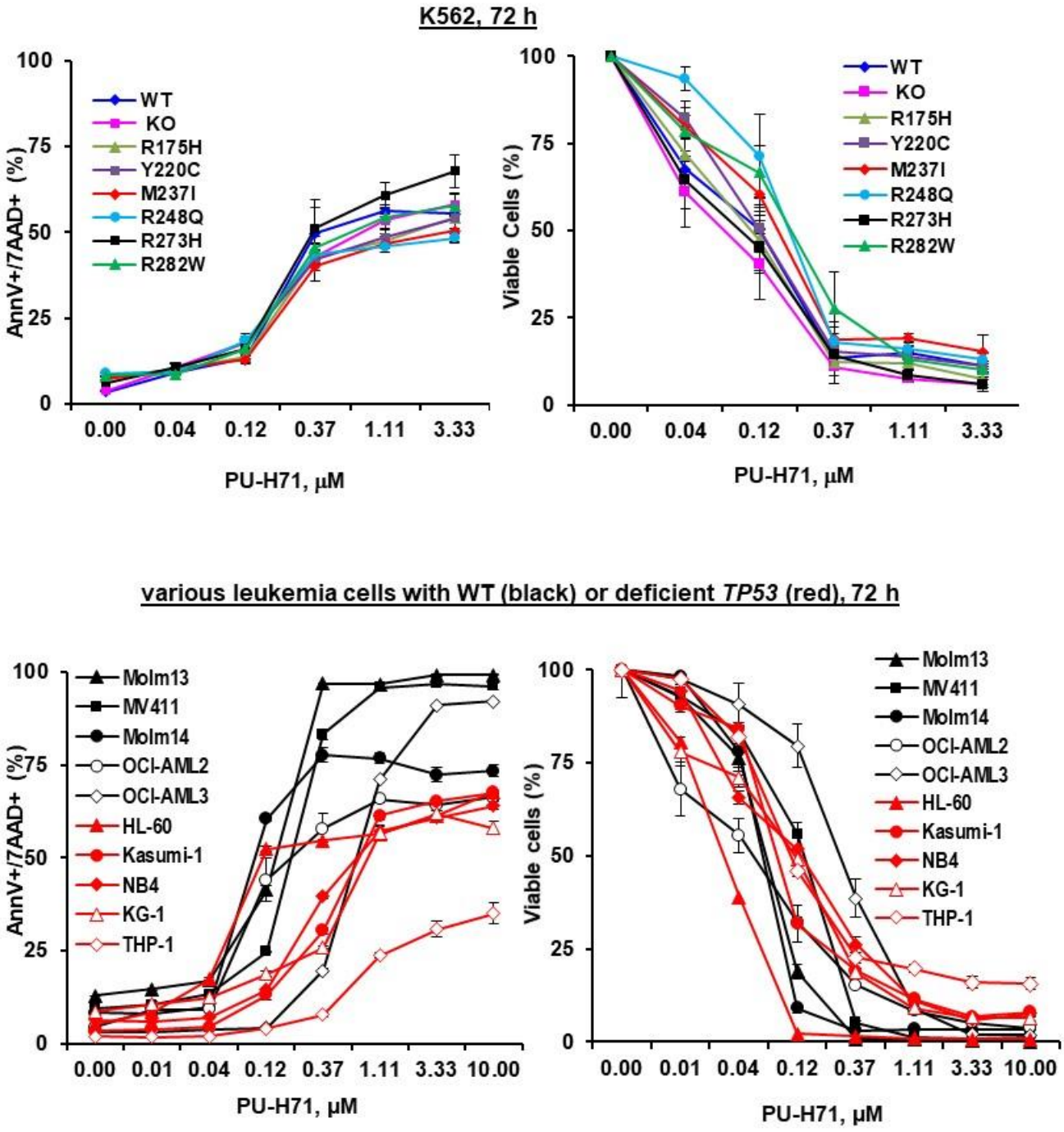

Supplemental Figure S2. PU-H71 effectively induces the death of *TP53*-mutant leukemia cells. *TP53*-WT, -KO, and -mutant K562 cells and various leukemia cells were treated with PU-H71 for 72 h. Cell death and cell counts were determined by flow cytometry.

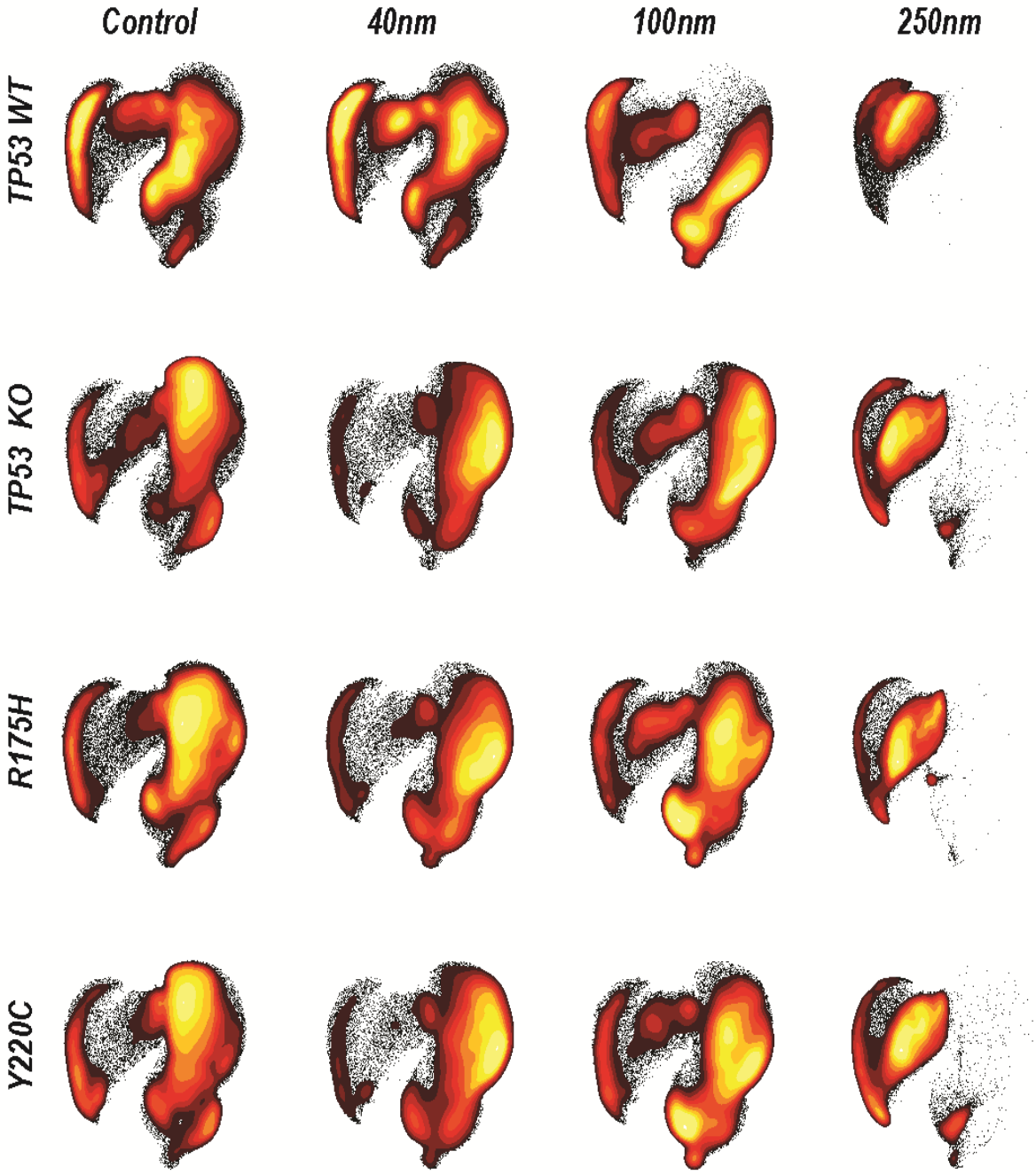

Supplemental Figure S3. The proteomic landscape of isogenic *TP53*-WT, -KO, and -mutant cell lines. Isogenic *TP53*-WT, -KO, and -mutant (R175H and Y220C) Molm13 cells were treated with 40, 100, or 250 nM PU-H71, and untreated cells were used as control. Cells were then subjected to UMAP dimension reduction and projected on 2-dimensional plots. UMAP plots for the indicated conditions are shown.

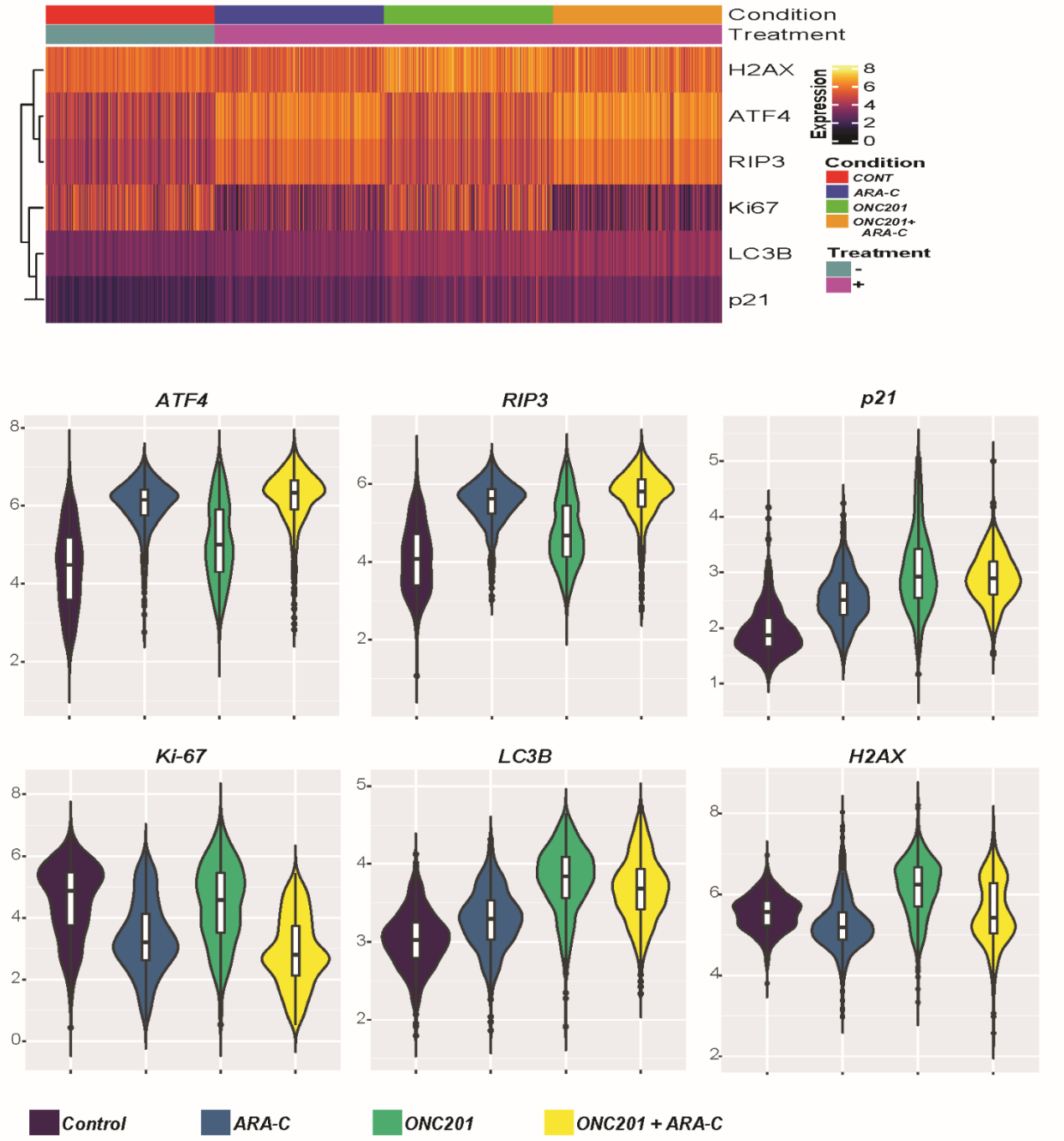

Supplemental Figure S4. The proteomic landscape of Leukemia cells treated with ONC-201, cytarabine, or both. *TP53*-WT Molm13 cells were treated with ONC-201, cytarabine, or both, and live cells were selected to generate a single-cell protein expression heatmap. The heatmap (top) shows the expression of the indicated markers (rows). Each column represents a single cell. The scale bar denotes scaled marker expression levels. Violin plots (bottom) show the expression of ATF4, RIP3, p21, Ki-67, LC3B, and γ-H2AX.

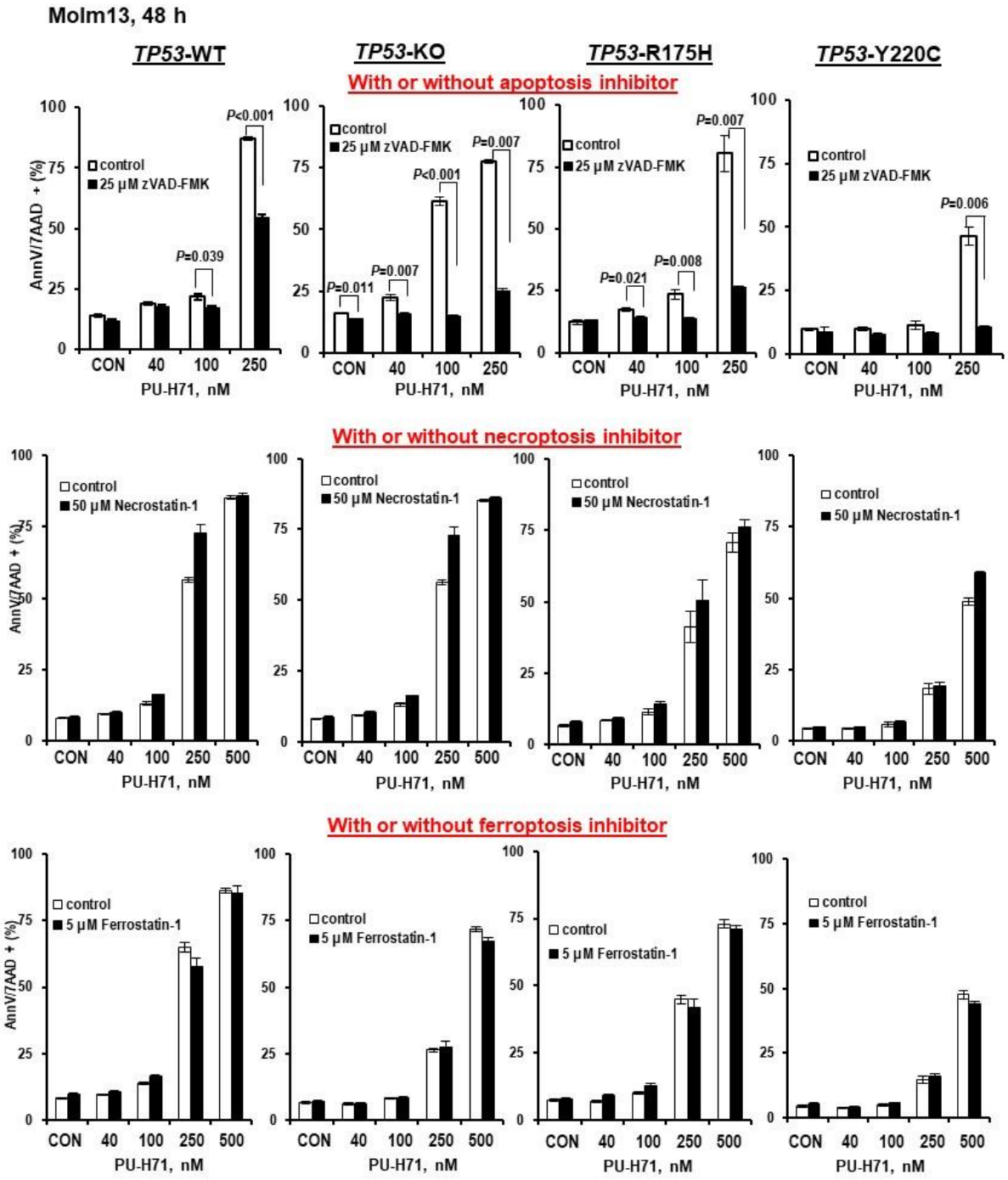

Supplemental Figure S5. PU-H71 induces primarily apoptotic cell death in AML cells independent of *TP53* status. Molm13 cells with *TP53*-WT, -KO, or mutations (R175H and Y220C) were treated with PU-H71 or PU-H71 with caspase inhibitor zVAD-FMK (25 μM), necroptosis inhibitor necrostatin-1 (50 μM), or ferroptosis inhibitor ferrostatin-1 (5 μM) for 48 h. Cell death was determined by flow cytometry. Cell death inhibitors were added to the cells 1 h prior to PU-H71 treatment.

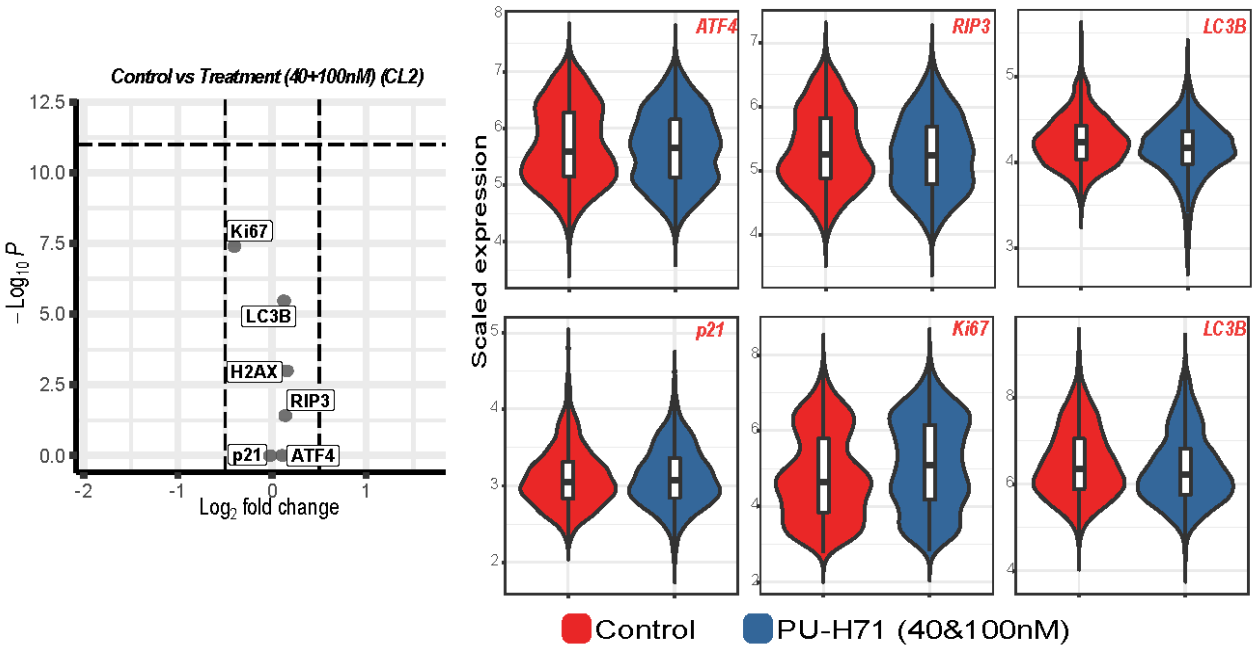

Supplemental Figure S6. PU-H71 marginally alters the proteomic profiles of CL2 cells. The CL2 cells, depicted in Figure 4A were filtered to select cells that were untreated and cells that were treated with 40 and 100 nM PU-H71. Differential expression analysis was performed, and the volcano was utilized to show proteomic differences between CL2 control cells and CL2 PU-H71 treated cells. Vertical dashed lines indicate the fold change cut-off of 0.5. Violin plots summarize the expression of indicated markers of CL2 untreated (red) vs PU-H71 treated (blue) cells.

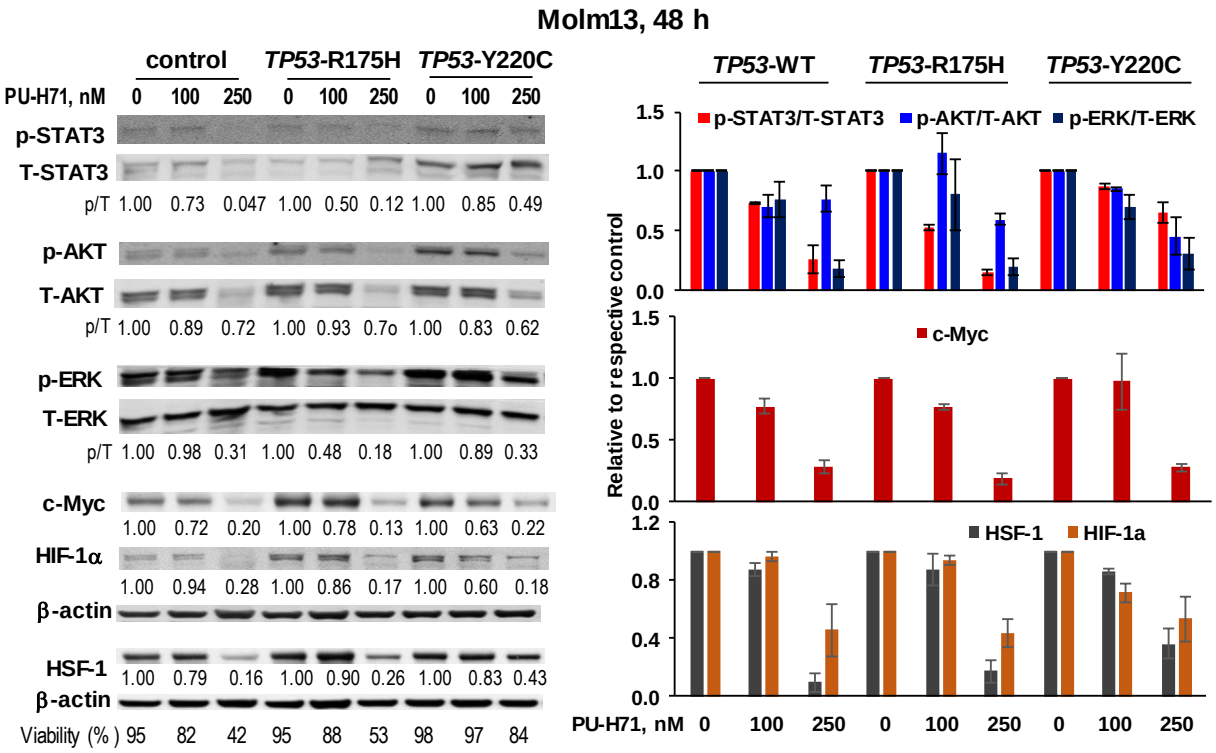

Supplemental Figure S7. PU-H71 decreases the levels of multiple signaling proteins and transcriptional factors in AML cells independently of *TP53* mutation status. *TP53*-WT and -mutant (R175H, Y220C) Molm13 cells were treated with PU-H71, and protein levels were determined by Western blotting.

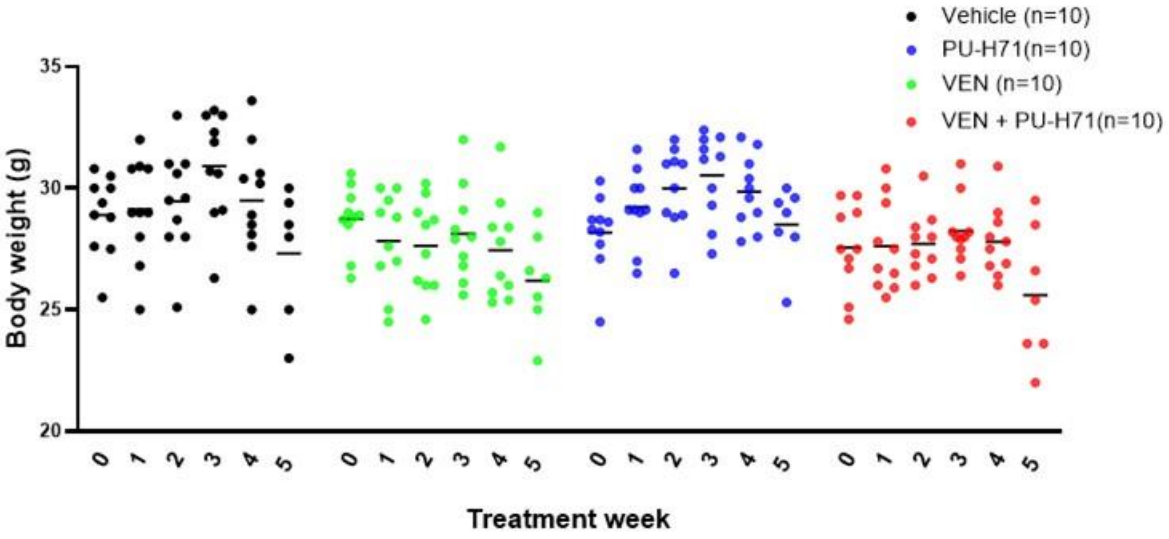

Supplemental Figure S8. Body weight of PDX-bearing NSGS mice during treatment.

Supplemental Table 1. Patient characteristics.

#	Blast %	Mutations	Previous treatment and responses	*In vitro* treatment
1A	88	***TP53*-R248W**	Relapsed AML. Resistance to fludarabine, high-dose cytarabine and filgrastim with or without idarubicin, cladribine, and **VEN**	PU
2	65	***TP53*-V173M**	Refractory AML. Resistance to azacitidine plus magrolimab	PU
14B	90	*BCORL1;MPL;STAT5; WT1;* ***TP53*-P152L**	Relapsed refractory AML. Resistance to azacitidine and **VEN**	PU
1B	59	***TP53*-R248W**	Relapsed AML. Resistance to fludarabine, high-dose cytarabine, and filgrastim with or without idarubicin, cladribine and **VEN**	PU+VEN
7	90	***TP53*-V272M**	Therapy-related-AML. Resistance to magrolimab, azacitidine, **VEN**	PU+VEN/FITC-PU
8	91	*NRAS;****TP53*-H179Q**	Resistance to azacitidine plus **VEN**, flotetuzumab	PU+VEN/FITC-PU
9	78	*CALR;DNMT3A;* ***TP53*-E171**	Relapsed refractory AML	PU+VEN/FITC-PU
10	60	*DNMT3A;IDH2;* ***TP53*-R175H**	Relapsed refractory AML to cladribine with idarubicin and cytarabine, **VEN**, cladribine, idarubicin, and cytarabine, **VEN**, decitabine and enasidenib.	PU+VEN/FITC-PU
11	83	***TP53*-S215T**	Therapy-related AML. Resistance to magrolimab, azacitidine, **VEN**	PU+VEN/FITC-PU
12	73	*DNMT3A;NRAS;* ***TP53*-R283fs**	Relapsed AML. Resistance to azacitidine plus **VEN** maintenance, fludarabine plus cytarabine	PU+VEN/FITC-PU
13	86	***TP53*-Y236L**	Relapsed refractory AML. Resistance to magrolimab, azacytidine, **VEN**, **PU-H71**	PU+VEN/FITC-PU
14	71	*BCORL1;MPL;STAT5; WT1;****TP53*-P152L**	Relapsed refractory AML. Resistance to azacitidine and **VEN**	PU+VEN
15	72	*CREBBP; IDH2; PTPN11; RUNX1; SRSF2*	Resistance to enasidenib+azacitidine, **VEN**+azacitidine, Omacetaxine+**VEN**	FITC-PU
16	85	*ASXL2; CSF3R; GATA2; KRAS; RUNX1; SF3B1*	Resistance to FHD-286	FITC-PU
17	87	*JAK2;RUNX1;TET2*	Relapsed/refractory AML. Resistance to cladribine and low-dose cytarabine, fludarabine and cytarabine plus **VEN**	FITC-PU
18	65	*BCOR;ETV6;EZH2;NRAS;PTPN11;RUNX1;SETBP1*	Relapsed/refractory AML. Resistance to **VEN** and cedazuridine-decitabine	FITC-PU
19	85	*DNMT3A; FLT3-ITD; IDH2 NPM1*	Resistance to cladribine with idarubicin and cytarabine, **VEN** and gilteritinib	FITC-PU
20	63	*ASXL1, CEBPA, SRSF2, TET2, STAG2*	Resistance to cyclophosphamide and fludarabine, tocilizumab and pentamidine	FITC-PU
21	56	*NRAS ;TET2;* ***TP53*-S94**	Resistance to azacitidine, cladribine and low-dose cytarabine, CLIA and gemtuzumab, azacitidine+**VEN**, **VEN**+CPX-351	FITC-PU
22	91	*CEBPA;DNMT3A;KRAS;****TP53*-P190fs**	Resistance to cladribine and cytarabine, alternating with decitabine	FITC-PU
23	97	*ASXL1;JAK3;NF1;RUNX1;SRSF2;TET2*	Newly Diagnosed	FITC-PU
24	96	*DDX41;ETV6;KRAS;SF3B1;RAD21*	Resistance to fludarabine+cytarabine, **VEN**+CPX-351	FITC-PU
25	72	***TP53*-C238Y**	Newly Diagnosed	FITC-PU
26	53	*ASXL1;RUNX1;SETBP1;U2AF1*	Resistance to vibecotamab	FITC-PU
27	63	*ASXL1;RUNX1;TET2;WT1*	Newly Diagnosed	FITC-PU
28	75	***TP53*-L43fs**	Resistance to IO-202 and azacitidine, ONC201	PU+VEN/Ki-67 colony assay
29	95	***TP53*-C242Y**	Resistance to CFI-400945	PU+VEN/Ki-67
31	85	*NF1, CEBPA, KDM6A,* ***TP53*-splicing?**	Resistance to VEN and PLX51107 + azacitidine.	PU+VEN/Ki-67 colony assay
32	90	*NF1,* ***TP53*-C135G,** *DNMT3A*	Newly Diagnosed.	PU+VEN/Ki-67 colony assay

#, sample number; VEN, venetoclax; PU, PU-H71

Supplemental Table 2. List of compounds used in the drug screening, their targets, and responses of the cells to the drugs (attached excel).

Supplemental Table 3. Western blot antibody source

	Antibodies	Sources	Catalog numbers
1	p-STAT3	Cell Signaling Technology	9145s
2	T-STAT3	Cell Signaling Technology	9139
3	p-AKT	Cell Signaling Technology	9271L
4	T-AKT	Cell Signaling Technology	2920
5	p-ERK	Cell Signaling Technology	4695T
6	T-ERK	Santa Cruz Biotechnology	sc-16565
7	MCL-1	Cell Signaling Technology	94296
8	BCL-XL	Cell Signaling Technology	2764S
9	BCL-2	Dako/Agilent	M088729-2
10	BIM	Abcam	ab32158
11	BAX	sigma	B8554
12	BID	Cell Signaling Technology	8762
13	BAD	Abcam	
14	BAK	Novus Biologicals	NBP1-74026
15	PUMA	Abcam	ab186917
16	HSF-1	Cell Signaling Technology	4356S
17	HIF-1α	BD Bioscience	610958
18	HSP90	Santa Cruz Biotechnology	sc-7947
19	p53 (Do-1)	Santa Cruz Biotechnology	sc-126
20	c-Myc	Cell Signaling Technology	5605

Supplemental Table 4. Combination index (CI) values of primary patient samples treated with PU-71 and venetoclax combination. Peripheral blood cells from AML patients were co-cultured with MSCs and then treated with PU-H71, venetoclax, or both for 48 h. Cell death was determined by flow cytometry. CI values were determined using CalcuSyn software and expressed as mean CI values of ED_{50}, ED_{75}, and ED_{90} ± standard deviations.

	Cell populations		
#, sample number	$CD45^+$	$CD34^+CD38^+$	$CD34^+CD38^-$
1B	0.160 ± 0.060	0.110 ± 0.070	0.593 ± 0.233
7	0.482 ± 0.035	0.335 ± 0.294	
8	0.078 ± 0.021	0.031 ± 0.039	
9	0.064 ± 0.056		
10	0.273 ± 0.062		
11	0.024 ± 0.019	0.003 ± 0.003	
12	0.001 ± 0.001	0.000 ± 0.000	0.016 ± 0.022
13	0.030 ± 0.027	0.009 ± 0.010	0.017 ± 0.014
14	0.014 ± 0.013	0.018 ± 0.013	

References

1. Boettcher S, Miller PG, Sharma R, et al. A dominant-negative effect drives selection of TP53 missense mutations in myeloid malignancies. *Science*. 2019;365(6453):599-604.
2. Seashore-Ludlow B, Rees MG, Cheah JH, et al. Harnessing Connectivity in a Large-Scale Small-Molecule Sensitivity Dataset. *Cancer Discov*. 2015;5(11):1210-1223.
3. Hafner M, Niepel M, Chung M, Sorger PK. Growth rate inhibition metrics correct for confounders in measuring sensitivity to cancer drugs. *Nat Methods*. 2016;13(6):521-527.
4. Muftuoglu M, Li L, Liang S, et al. Extended live-cell barcoding approach for multiplexed mass cytometry. *Sci Rep*. 2021;11(1):12388.
5. Butler A, Hoffman P, Smibert P, Papalexi E, Satija R. Integrating single-cell transcriptomic data across different conditions, technologies, and species. *Nat Biotechnol*. 2018;36(5):411-420.